electronics

MDPI

Review

Different Antenna Designs for Non-Contact Vital Signs Measurement: A Review

Carolina Gouveia [1,2,†], Caroline Loss [3,†], Pedro Pinho [1,4,*,†] and José Vieira [1,2,†]

1 Instituto de Telecomunicações, 3810-193 Aveiro, Portugal; carolina.gouveia@ua.pt (C.G.); jnvieira@ua.pt (J.V.)
2 Departamento de Eletrónica, Telecomunicações e Informática, Universidade de Aveiro, 3810-193 Aveiro, Portugal
3 FibEnTech Research Unit, Universidade da Beira Interior, 6200-001 Covilhã, Portugal; carol@ubi.pt
4 Departamento de Engenharia Eletrónica, Telecomunicações e de Computadores, Instituto Superior de Engenharia de Lisboa, 1959-007 Lisboa, Portugal
* Correspondence: ptpinho@av.it.pt
† These authors contributed equally to this work.

Received: 30 September 2019; Accepted: 1 November 2019; Published: 6 November 2019

Abstract: Cardiopulmonary activity measured through contactless means is a hot topic within the research community. The Doppler radar is an approach often used to acquire vital signs in real time and to further estimate their rates, in a remote way and without requiring direct contact with subjects. Many solutions have been proposed in the literature, using different transceivers and operation modes. Nonetheless, all different strategies have a common goal: enhance the system efficiency, reduce the manufacturing cost, and minimize the overall size of the system. Antennas are a key component for these systems since they can influence the radar robustness directly. Therefore, antennas must be designed with care, facing several trade-offs to meet all the system requirements. In this sense, it is necessary to define the proper guidelines that need to be followed in the antenna design. In this manuscript, an extensive review on different antenna designs for non-contact vital signals measurements is presented. It is intended to point out and quantify which parameters are crucial for the optimal radar operation, for non-contact vital signs' acquisition.

Keywords: antennas; radar; vital-signs; CW; UWB

1. Introduction

The ability to measure physiological signals accurately has several applications in different areas, from health care to the full medicine procedures. Here, the main vital signals include breathing and heart rate. By combining this concept with the consumer demand for flexible and wireless sensors, it is possible to have a positive impact on society and open a new door in the health care industry.

Until now, the conventional measuring equipments are directly in contact with the subject, which requires some wires' usage. For this reason, the research in this area is focused on the development of solutions with a high degree of freedom, robustness, and obviously maintaining the same accuracy. One possible solution is to use wearable sensors in contact with the subject body, although this solution is more evasive and not comfortable. In this sense, the concept of bio-radar has emerged. The bio-radar uses the Doppler radar principle to evaluate the breathing and heart rate of a subject in a convenient contactless way. It uses an antenna for transmission (TX), which focuses the energy towards the subject chest-wall, and another antenna for reception (RX), to acquire its reflection. This approach stands out as being more advantageous when compared to the traditional devices using contact sensors on the human body, since the subject can be remotely monitored.

The antenna design plays a crucial role in the performance of bio-radar system, in order to obtain the best signal quality and to maintain a signal-to-noise ratio (SNR) at a superior level. Several types of antenna have been used in literature, covering a wide range of frequencies, polarization modes, and half-power beamwidths (HPBW), according to the application at hand. However, most of the papers related to non-contact vital signal (NCVS) measurement using radar-based systems, do not have the antenna information clearly detailed. Mostly, they focus on the global system performance, the main challenges that had to be overcome and new algorithms to extract the vital signs successfully. The majority of papers do not mention the design of the antennas and its importance in the global behavior of the system. Even though, articles that refer to antennas are focused on specific aspects that can enhance the main goal of those works.

Antennas can be designed as single elements or in array configuration, using conventional or alternative materials, depending on the final application. Moreover, in the industry framework, selection of the proper parameters should be done with care, aiming to search for portable solutions (decrease the system size) and using low cost materials that are also able to keep the optimal antenna performance. Therefore, there is a need to review the antenna side, in order to seek which are the best antenna characteristics to properly apply in radar systems for vital signs' acquisition.

In [1], a preliminary investigation on the best antenna features for bio-radar applications was made. This paper was the only review work related with the antennas impact that we have found so far, and the authors also mentioned the lack of reviewing on this matter and in which way this is important. Their study encompasses different antenna designs, which have features for different applications. The authors conclude that increasing frequency has many advantageous aspects, since shorter wavelength helps on decreasing the antennas size, and are more sensitive to low amplitude motions (for example, it could improve on the cardiac signal detection). They have also presented a comparative table that shows a higher gain for these designs.

In our work, it is intended to review the state-of-the-art on antennas for NCVS monitoring, namely for respiratory and cardiac signals. Different frequencies and radar operation modes will be explored, as well as the different designs, and several implementation examples are also presented and discussed. By gathering this information, it is intended to determine which are the antenna features that are more suitable for NCVS acquisition, such as directivity, gain, or polarization. Moreover, it is also intended to present a panoply of low cost substrates and efficient antennas integration that can contribute to system portability and low-profile. It is important to note that different applications and environments require different characteristics, but the goal of this manuscript is to define common guidelines that are required to be maintained for any optimal system performance.

This manuscript is divided as the following: first of all, bio-radar theory is briefly presented in Section 2. In this section, different radar operation modes are also introduced. Then, Section 3 presents some antenna examples developed mainly for Continuous Wave (CW) radar. This section is sub-divided according to the different goals of the authors. Similarly, Section 4 presents more antenna solutions but focused on Ultra-Wideband (UWB) radars. Section 5 presents a briefly summary and discussion about the characteristics of the antennas developed for bio-radar applications. Moreover, a group of trade-off decisions to design the most suitable antenna for bio-radar applications is presented, based on the review made. Finally, conclusions and guidelines are presented in Section 6.

2. Bio-Radar Theory

The bio-radar system can measure vital signs using electromagnetic waves. The operation principle of this system is based on the Doppler effect, which relates the received signal properties with the distance change between the radar antennas and the person's chest-wall [2]. The frequency change on the received signal, caused by the motion of the chest-wall, depends on the total number of wavelengths in the two-way path, between the radar and the target that can be determined through (1):

$$N_\lambda = \frac{2R}{\lambda}, \tag{1}$$

which is given in waves per second (Wave/s) and where R is the radar range and λ is the wavelength of the transmitted signal.

Considering that the radar is located in a fixed position, the same frequency is received over the time if the target is also stationary because the same number of N_λ is received. However, if the target moves toward or away from the radar, different frequencies are received: if the motion is toward to the radar, higher frequency is received due to the bigger number of received N_λ. On the other hand, if the target is moving backwards, a lower frequency is perceived, due to the fewer number of received N_λ [3].

The frequency shift effect can also be perceived as phase change, once each wavelength corresponds to a phase change equal to 2π. Thus, if the path travelled by the wave changes due to the target's motion, also the number of N_λ changes, hence the total phase change relative to range R is given by the Equation (2):

$$\phi = 2\pi N_\lambda. \tag{2}$$

The Doppler radar is the basis of some radar operation modes, namely the Continuous Wave (CW) radar or the Ultra-Wideband (UWB) radar, as depicted in Figure 1. Their operation principle influences the antennas specification directly. In the next sections, a brief introduction about radar operation modes is presented for contextualization purposes.

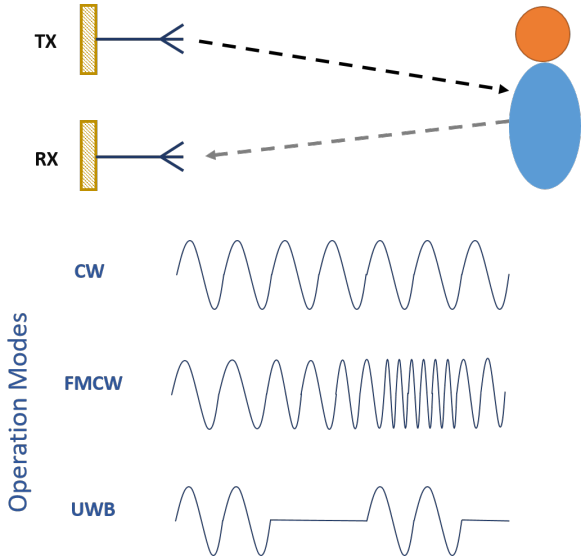

Figure 1. Doppler radar applied to vital-signs acquisition, using different operation modes.

2.1. Continuous Wave Radar

CW radar transmits and receives a radio-frequency (RF) signal continuously. Usually, the transmitted signal is defined as a single-tone. A radar system that uses this operation mode is composed of a signal generator, to generate the signal for TX and also to down-convert RX signal on the receiver side. Once the system usually handles with narrow band signals, it is possible to perceive the frequency shift due to the Doppler effect when the target is moving. Thus, CW radar can measure the velocity of the target's motion, and this feature allows for distinguishing between a moving target from stationary objects, independently of their distance (within the radar's range) [4].

CW radar presents a significant advantage regarding the implementation complexity. It uses a single oscillator for both TX and RX, and the filters used in the receiver chain can be quite simple because TX and RX signals have a narrow bandwidth.

Nonetheless, some disadvantages can be pointed out about this type of Doppler radars. Once TX and RX are continuous operations, due to circuitry or antenna coupling, a portion of the transmitted signal can directly affect the signal at the receiver causing leakage [3]. Moreover, the clutter from

multiple reflections of stationary objects located within the range can contribute to the signal power, generating low frequency noise and DC offsets.

Frequency-Modulated Continuous Wave Radar

Frequency-Modulated Continuous Wave (FMCW) allow the computation of the target's velocity and distance between the target and the radar, once it has more range resolution that does not exist for a single frequency waveform [4].

In this operation mode, frequency modulation is performed, usually with a triangular modulation in order to increase and decrease the frequency linearly over time.

Then, another triangular signal is the received signal, which is the delayed version of the transmitted one, and the delay can be quantified by $T = 2R/c$ s, with R being the radar range and c the speed of light. The modulated signal bandwidth determines the accuracy of the range measurement, and the modulation rate determines the maximum detectable range without ambiguity. The mix between the transmitted and the received signals result in a frequency difference f_r that changes according to the target motion, and from where the vital signs are extracted.

2.2. Pulsed Radar

Pulse radar transmits pulsed bursts and then listens to the resultant echoes. In contrast with the previously mentioned radars, TX and RX operations are not done simultaneously. Therefore, the pulse repetition period should be longer than the round-trip path length of the transmitted wave, to receive the echoes between transmissions [5].

Since the reflections are not acquired at the same time as the signal's transmission, the leakage from the transmitter and the parasitic reflections are separated temporally from the long-range targets. This means that, as we have to wait for the full transmission, the reflections that occur immediately from short-range objects are not detected, which represents a clear advantage when comparing to the CW radar. Similarly to the FMCW radar, it is possible to measure the target range.

On the other hand, the pulsed radar is more complex to implement [5]. Moreover, there is a lack of velocity resolution, which implies a limit in target's velocity.

Ultra-Wideband Radar

UWB radar is a special application of the pulsed radar since very short duration pulses are generated, performing wide bandwidth signals. The Federal Communications Commission (FCC) has established that a signal can be categorized as a UWB signal if it has a bandwidth equal to or higher than 500 MHz [3].

The operation of UWB radars starts by generating short pulses and transmits them through the antenna. Then, the target will reflect a portion of the transmitted signal. The total range ΔR of this radar is given by the Equation (3) [6]:

$$\Delta R = \frac{c}{2 * BW} = \frac{\tau c}{2}, \tag{3}$$

where BW is the bandwidth of the radar pulse in frequency domain and τ the bandwidth in time domain. With this type of radar, it is possible to compute the distance to target d_T (Equation (4)):

$$d_T = \frac{\Delta t * c}{2}, \tag{4}$$

where Δt is the delay between the transmitted and the received signal.

Applications of the UWB radars encompass motion detection beyond different materials, due to the vast panoply of different wavelengths that can be used. With this type of technology, it is possible to perceive periodic or quasi-periodic motions because they cause periodic changes in the received signal.

This periodic change is reflected across multiple scans, which are then compared with a reference scan in order to locate the target.

3. Antennas for CW Operation Mode

Generally, designing an antenna is a challenging task, since it is made by following a guideline based on a group of trade-off decisions. The optimal performance of the antenna can be dictated by an infinite gain, lack of side or back lobes, infinite S_{11}, among many other characteristics. However, these features should also be achieved having in mind specific restrictions and requirements regarding the application at hand. In the framework of NCVS applications, this care must also be accounted due to the system sensitivity to environmental clutter, to the very limited radar cross-section (RCS) and to the lowpass signal characteristics.

Although there are multiple antenna types, shapes, and layouts that can be combined in order to fulfill those trade-off decisions, there is not a single solution once the carrier frequency of the transceiver and its operation mode largely influence the antenna behavior. The transceiver operation mode (such as CW, FMCW, or UWB) also depends on the application of the bio-radar. For example, applications that aim to distinguish between different individuals, i.e., where there are multiple subjects to monitor, can use FMCW technology, since the usage of chirps can help to indicate the subject location. Furthermore, rescue applications imply that electromagnetic waves cross obstacles. For this purpose, ultra-wideband front-ends are more indicated. Finally, if the goal is to monitor bedridden patients, CW is enough and the hardware and signal processing are less complex.

In this section, some examples of different antenna designs are presented, considering the CW operation mode. The examples are subdivided in different antenna characteristics according to the improvement goal of authors.

3.1. Directivity

Taking into account the CW operation mode, a system performance evaluation was made in [7]. Considering four different antennas, all operating at 2.4 GHz, several tests were performed inside an anechoic chamber, where the vital signs of a subject were monitored using the following antenna types and their respective beamwidths:

1. Single patch antenna $\Rightarrow 92^\circ$;
2. Yagi antenna $\Rightarrow 47^\circ$;
3. Log-periodic antenna $\Rightarrow 62^\circ$;
4. Helical antenna $\Rightarrow 49^\circ$.

The radiation pattern of each antenna was verified individually before the experiments. Wide beams are susceptible to acquire more clutter and noise, hence narrower beams are preferable. Taking this into account, among the four tested antennas, Yagi and Helical were the ones that have narrower radiation patterns, and they also have identical values of HPBW. Moreover, they are low cost alternatives. However, a Yagi antenna does not have a symmetrical beam across E- and H-planes unlike the Helical antenna.

The influence that the pair TX/RX can have on each other is also studied, by checking the radiation pattern with another antenna by its side (antennas' feeding points were 24 cm apart). The authors concluded that the influence is minimal, as long as TX and RX antennas are at least a wavelength apart.

The experiment results showed that the error in signal rate computation was smaller for helical antennas. The authors believe that the optimal performance is directly related to the directivity and symmetry in E- and H- planes. An additional test was performed by equalizing the gain for all antennas and repeating the vital signs measurement. Helical antennas stand out again, the beat rate was computed accurately, and the Signal-to-Noise-plus-Interference Ratio (SNIR) increased.

One of the first usages of helical antennas for NCVS acquisition was proposed in [8]. In this work, two antennas with 4-turns and, therefore, directive beams ($\approx 40^\circ$ of HPBW) were used to acquire

vital signs in non-stationary environments, such as vehicles. Compensation of motion artifacts was implemented through a differential measurement, using these antennas in separate. Antennas were designed to operate at different but near frequencies, namely, 2.46 GHz and 2.51 GHz, respectively. Both antennas were implemented with different linear polarization orientation to isolate each signal.

Helical antennas operating at 2.4 GHz are also proposed in [9]. More specifically, the axial-mode helical antenna design was implemented, with an 8-turn design and a simple matching process to feed the antenna without increasing its total size. Helical antennas operating at axial mode are known for having high directivity and hence high gain, which also enables more detection range. Nonetheless, to build a helical antenna for NCVS acquisition, a trade-off should be respected, since the radiation pattern is as directive as the number of turns. Therefore, for a highly directive antenna, a larger size antenna is required. The work presented in [9] resulted in a 8-turn antenna with 20 cm length, HPBW equal to 44.6° and gain equal to 9.80 dBi. Moreover, these antennas also have circular polarization to achieve better SNIR and thus better accuracy on detecting vital signs.

Finally, in [9], the performance of a 1-turn helical antenna was compared with a single patch antenna. Both antennas were operating at 2.4 GHz and had the same HPBW (around 60°). Comparison results showed that helical antennas have more gain, up to 2 dB above the one from a single patch antenna.

Besides helical antennas, any antenna design that can provide directivity can be advantageous for bio-radar systems. In [2], an antenna evaluation is done, by comparing the performance of the antenna array operating at 5.8 GHz with the performance of a single patch operating at 2.5 GHz. As mentioned previously, array antennas have a directive beam, which focuses the radiated energy on the subject chest-wall. On the other hand, a single patch has a wider beamwidth and radiates in different directions, hence the received signal has more noise from the clutter and parasitic reflections. By taking into account these issues, the comparison mentioned above was made by estimating the DC component of each signal acquired with each antenna. The authors concluded that the signal acquired with a single patch has a higher DC component rather than the one acquired with a narrower beam.

Customized Directivity

Until now, we have seen that narrow radiation patterns are preferable to focus all the energy on the desired target. However, some applications require different beamwidth customization to cover the area of interest. For example, in [10], a one-dimensional patch array is developed to measure vital signs from elderly people located in a room. The antenna has to be designed so its beamwidth can cover the full room. The radar front-end was located in the middle of the room, using a microstrip patch antenna array, operating at 24 GHz. The radiation pattern is defined as a triangle-shaped with $\pm 33.7°$ opening angle, in order to illuminate the corners of the room. On the final prototype, it is intended to use a standard patch array, beamshiped on the H-plane used as a TX antenna and a linear-array, beamshiped on the E-plane used as an RX antenna, with 10-dB gain higher for the $\pm 33.7°$ angle than for the 0° angle. In this way, multiplication of both radiation patterns will rectify power losses in corner spots.

The antenna array proposed in [10] corresponds to the RX antenna beamshiped on the E-plane. In summary, the designed antenna is an array with three microstrip patch resonators fed in series through a microstrip line, where the last patch is a single-port standard patch. Patches are optimized to operate at 24.125 GHz and are built using an RO4835 substrate, with a relative permittivity of $\varepsilon_r = 3.66$. The total array length is equal to 15.694 mm and a width equal to 6.339 mm. In the simulation, it was possible to achieve the required features respecting to radiation pattern, with 8 dB higher gain at 33.7°. The measurements meet the specifications, but the authors state that there are some improvements that need to be done.

3.2. Different Carrier Frequency Applications

The usage of high carrier frequencies increases the sensibility to detect imperceptible target motions. Planar microstrip antennas tuned at these frequencies enable the on-chip integration for

portable applications. For example, in [11], a circularly polarized (CP) 2 × 2 patch array antenna is presented, to be further integrated with a 60-GHz Doppler radar. The low-temperature co-fired ceramic (LTCC) substrate is used to increase bandwidth, which is also crucial for single-tone applications to guarantee good performance in the case of manufacturing issues.

Another millimeter-wave microstrip array antenna was presented in [12], but with a lower operating frequency, 24 GHz. The antenna was developed to evaluate the organism adaption to physical and mental stress remotely. Each antenna element from the transmitter and receiver array is single-patch antenna U-slot shaped. The TX array included 16 elements (8 × 2 array) for a narrow beam, and the RX was composed by 48 elements (8 × 6 array) for a large aperture area. Each single-patch is fed using a power divider network to adopt an unequal current amplitude distribution instead using an equal amplitude. The antenna module was designed using FR-4 substrate, with $\varepsilon_r = 3.55$, and copper cladding for the conductive pats. The final dimensions of the antenna module were 73×64 mm^2. This paper presents only the simulation of these antennas and the numerical results obtained were: bandwidth 24–25 GHz (RX) and 23.3–23.7 GHz (TX); S_{11} less than -10 dB for both TX and RX antennas, and a gain equal to 17.15 dBi for the TX antenna, while the RX antenna exceeds 17 dBi. The mutual coupling was below -35 dB at 24 GHz, providing good isolation between the TX and RX antennas.

Later, in 2016, the same research group has proposed a new microstrip array antenna, operating at 77 GHz, to be used as TX and RX antennas, in a bio-radar module [13]. The array is composed by 160 single-patch elements (16 × 10) for a narrow beam, which are fed using a power divider network. The antenna module was designed using an RO3003 substrate, with $\varepsilon_r = 3.0$, and copper cladding for the conductive parts. The final dimensions of the antenna module were 43.79×25.04 mm^2. The simulated S_{11} showed that the antenna is capable of operating between 74.6 GHz and 79.7 GHz, having a bandwidth equal to 5.1 GHz. At 76.5 GHz, the calculated gains on the H- and E-plane are higher than 25 dBi, and the HPBW on both planes is 12°. In addition, in this frequency, the side lobe level is -12.5 dB and -11.5 dB for the H- and E-plane, respectively. The numerical results prove that this array module can be used for bio-radar applications.

In addition, a continuous wave harmonic radar system is presented in [14]. The system is composed of two slot array antennas designed using a Substrate Integrated Waveguide (SIW) technique, to operate at 12 GHz and 24 GHz. The SIW slot array antennas had 13 dBi and 24 dBi of gain, for the 12 GHz and 24 GHz, respectively. The experimental results show that, by using harmonic radar, the received signal power can be increased while the noise level decreased. Regarding the sensitivity of the system, as expected, the detection of vital signs was possible when the noise level was below the received signal power.

On the other hand, low carrier frequencies can also be interested to be explored, since they allow high EM penetration in the human body and thus increase accuracy in vital sign detection. In [15], a fractal-slot patch antenna operating at 915 MHz and combined with an ultra-wideband Low Noise Amplifier (LNA) was used for this purpose. In order to evaluate the performance of this CW Doppler radar operating with such low frequency, the path losses were computed and compared for 915 MHz and 2.45 GHz signals, when propagating in the subject body that was located 80 cm apart from the radar. The authors could conclude that, with the 915 MHz radar, it was possible to achieve signals with more information. For example, the cardiac signal achieved a 7 dB superior level for 915 MHz radar rather for 2.45 GHz.

A fractal-slot patch antenna design, using FR-4 substrate $\varepsilon_r = 4.4$ and 1 mm thickness, helped to decrease the antenna size and also increase the path length of EM wave, keeping the antenna performance. The final patch size was equal to 70.4 mm, which is 7.9% smaller than a conventional patch. Moreover, the total physical size reduced 15.2% when compared with a conventional patch antenna operating at the same frequency. The fractal slot in the center of the patch was implemented using Koch snowflake patterns to increase the surface current on the patch. The patch was designed with truncated edges to achieve circular polarization. The obtained performance characteristics were

26 dB of return loss, 17 MHz of bandwidth, HPBW equal to 108°, 12% of radiation efficiency, and 5.8 dBi of gain. The total antenna size was 140.8×140.8 mm^2.

As seen in the examples presented in this sub-section, the carrier frequency also influences the antenna size. Although, due to some hardware limitations, using high frequency carriers can not be always an option; therefore, other solutions will be explored to optimize the size of the radar system and are discussed in the next sub-section.

3.3. Techniques to Reduce the Antenna/System Size

Usually, two separate antennas are used to perform TX and RX. However, they have to be separated at least a half-wavelength to avoid mutual coupling, which increases the total size and hampers the antenna integration in more compact systems [16]. One alternative to decrease size is using a single antenna, but this should be done with care. The most obvious way to separate TX and RX signals is using circulators, although they are composed by ferrite materials, have a fixed size and are costly components [16,17]. The other option is to use couplers, but they divide signal power, and at least 6 dB of power loss is induced. Nonetheless, a dual-antenna is still an option if antenna design techniques are applied specifically to reduce the antenna size. Below, we describe some works that present techniques to reduce the size of the antennas for bio-radar.

3.3.1. Single Antenna for TX/RX

Although the authors do not mention the radar operating mode, in [18,19], they proposed a single antenna for TX/RX. In [18], a low cost system using a Yagi patch antenna as a single antenna for the RF front-end was planned. The Yagi patch antenna has a simple structure, is discreet, and has a highly directive lobe. The antenna was developed using FR-4 substrate, with relative permittivity $\varepsilon_r = 4.4$ and a total size of 120×80 mm^2. The achieved performance parameters were $S_{11} = -22.87$ dB at 2.45 GHz and gain equal to 8.69 dBi and a minimal back lobe (-10.50 dB). Since a single antenna was used for both TX and RX, the separation of the incoming and outcoming signals was performed by a circulator.

Similarly, a transceiver with a single antenna was also implemented in [19]. In this case, a horn antenna operating in the V-band (50–75 GHz) was used, with 25 dBi gain and beamwidth equal to 7°. A circulator with 18 dB isolation was used for TX and RX signals separation. This amount of isolation was not sufficient to avoid leakage at the receiver stage, hence a clutter canceller was also implemented and it is explained in detail in [19].

As seen so far, when the transceiver has a single antenna for TX and RX, a circulator is used to separate signals. Although this hardware component is costly, has large dimensions, and sometimes it is not as effective as demonstrated in [19]. Therefore, alternative solutions for single antenna implementation can be explored. One possible solution is sharing the same radiating aperture using a CP antenna and using opposite polarizations for TX and RX functions [16,17,20,21]. For example, in [17], a single antenna with CP and operating at 24 GHz, was shared by TX and RX. Different polarization directions were used, more specifically left-hand circular polarization (LHCP) for TX and right-hand circular polarization (RHCP) for RX. A quadrature coupler (Langer coupler) was also used to avoid the circulator usage, and TX and RX were located in opposite ports. The full radar system size was 4×4 cm. It was tested by acquiring vital signs at a distance of 50 cm. An average of 21 beats/min and 69 beats/min was detected for respiration and heartbeat rate, respectively.

A similar solution was presented in [16], this time using a radar front-end operating at 2.4 GHz. The antenna is composed by three metallic layers wrapped in FR-4 substrate with 50 mm of diameter. The bottom layer is a ring-shaped quadrature hybrid coupler (QHC) for the vias' excitation. The middle layer is the ground plane and the top layer is a circular patch fed with two vias, for TX and RX, respectively. This layout was selected to help reduce the total system size. With this sharing method using opposite polarization directions, it was possible to obtain 30 dB isolation between TX and RX.

Then, this antenna was used to monitor both heartbeat and respiratory signal accurately within a range of 60 cm.

The same approach was used in [20], where a bio-radar system is presented with a phase-locked loop and uses a single antenna for TX and RX. In this work, the authors have developed a circular-polarized annular ring microstrip antenna, with RHCP at transmitting mode and LHCP at receiving mode. This antenna was designed to operate at 2.4 GHz and presented an HPBW of 132°, and measured return loss of 20 dB. In further measurements, the radar was able to detect the respiratory signal of a human seated at 30 and 50 cm away from the radar. Later, in [21], the authors have made a study comparing this system with a 10 GHz bio-radar with separated antennas for TX and RX. The 10 GHz super-heterodyne bio-radar system is fully described in [22]. The TX and RX array presented a linear polarization, 8 dBi of gain, HPBW of 30°, and measured return loss of 30 dB. The vital signs of a subject were acquired from different distances, starting with 0.3 m until 2.9 m away from the radar. This measurements were performed with both systems [21]. Comparing the obtained results, the authors have concluded that, despite the advantages of the 10 GHz bio-radar (higher antenna gain and RCS), the system had not shown significant improvement compared to the 2.4 GHz bio-radar system. In addition, the 10 GHz bio-radar is more expensive and complex to implement.

Single antennas are indeed an alternative to decrease the front-end size. However, some drawbacks were identified. In [23], a test was performed to evaluate the system performance, using a single antenna or two separate antennas for TX and RX. Results showed that a single antenna has good accuracy in vital signs' detection, considering a short-range. The distance between the subject and the system antennas was equal to 5 cm, although two separated antennas could cover a wider range with the same level of signal quality. The subject was monitored successfully within the range of 25 to 200 cm. Antennas were located 20 cm apart from each other to avoid cross-talk effect.

In [23], the authors carefully selected the microstrip type of antenna for their experiments. Apart from having an acceptable gain, microstrip antennas can also be embedded on chip devices, which reduces the total size of the system and use a low-cost fabrication process. Moreover, microstrip antennas can be arranged in arrays to increase gain, decrease the side-lobe level, narrow the beamwidth, and thus focus the energy only on the target of interest. In this sense, three different microstrip antenna arrays of ultra-wide elements were designed and tested, and the following gains were achieved:

1. 2×1 elements $\Rightarrow \approx$13 dBi;
2. 3×3 elements $\Rightarrow \approx$16 dBi;
3. 6×2 elements $\Rightarrow \approx$18 dBi.

All of the antennas were designed to operate on a 60 GHz band, using Duroid substrate with $\varepsilon_r = 2.2$. The main purpose was to integrate these antennas in a CW front-end. However, antennas were designed with an ultra-wide band (57.24 GHz–65.88 GHz) to enhance the fabrication tolerance when embedding in a low cost printed circuit board (PCB).

In practice, it was possible to observe that the achieved bandwidth did not have an increased behavior in relation to the number of elements like the gain. In fact, it decreased with the number of elements in the array.

3.3.2. Size Reduction Techniques Applied with Dual-Antenna for TX and RX

Now, considering the dual-antenna option, other techniques were explored to reduce the antenna size as much as possible.

In [24], a 3D design was chosen to use as a portable life-detecting system. In this paper, the authors presented a 3D-orthogonal patch antenna that was designed to operate from 900 MHz to 12 GHz and was developed using FR-4 substrate, with $\varepsilon_r = 4.4$ and 1.2 mm of thickness. The antenna module is composed by the TX and the RX arrays, with 15 and 20 patch elements, respectively. The TX and RX arrays are connected together by a power splitter and power combiner. Comparing the simulated

(900 MHz to 12 GHz) and measured performances of both antennas for all bandwidth frequencies, the best results were from 800 MHz to 4.4 GHz for the TX and 9.4 GHz to 12 GHz for the RX antenna. As the authors have used only one average permittivity value ($\varepsilon_r = 4.4$) during the simulation, and the antenna covers an extra wideband; they concluded that the variation of the substrate permittivity at different frequencies has influenced the results.

The authors also tested the applicability of this extra wideband antenna for a Doppler radar system. The test was performed using a PNA-X in a non-controlled environment, where the subject was placed 80 cm away from the antenna. The measurements were carried out using five different frequencies (0.953 GHz, 2.198 GHz, 3.362 GHz, 5.556 GHz, and 10 GHz) and during 3 min. The system was more sensitive for higher frequencies. As for the go-through materials applications—such as finding survivors—lower frequencies are required, and similar measurements were made with a wood barrier (3 cm of thickness) between the subject and the antenna. In this case, in higher frequencies, the system was negatively affected because the amplitude of the signal at 5.556 GHz was 0.7 mm while at 3.637 GHz was 2 mm.

In [25], the authors combined two developed arrays with a commercial 24 GHz radar system chip in Silicon Germanium technology, reducing the size of the radar module. The TX and RX are 4×5 patch arrays, operating at 24 GHz, designed and fabricated using RO4350 with 0.254 mm and $\varepsilon_r = 3.48$, as a substrate. The simulated gain was about 17.1 dBi and the beamwidth was around 24° and 20° for the E- and H-plane, respectively. This compact radar module was tested by measuring the breathing and heartbeat of an adult seated 1.5 m away from the radar. In these conditions, the radar was able to measure 15 breath/min and 76 beats/min, which agrees with the results obtained with a pulse sensor (76 beats/min).

Furthermore, portable and low-power radar was designed and built on a palm-size PCB, and it is presented in [26]. In this work, the authors proposed two 2×2 printed patch antenna arrays, for 5 GHz, to be used as TX and RX antennas. The arrays had 9.7 dBi (at 5.8 GHz) of gain and HPBW equal to 20°. To compare the results, the measurements using a UFI1010 wired fingertip pulse sensor were also performed. In comparison, the heart rate accuracy obtained with the non-contact radar was 98.82%, 92.40% and 81.35% at 0.5 m, 1.5 m, 2.8 m away from the radar, respectively.

Techniques to integrate the radar in a complementary metal-oxide-semiconductor (CMOS) chip were explored in [27,28]. In [27], the authors have proposed a 5.8 GHz radar in a 0.18 µm CMOS chip. Generally, this on-chip integration is done for higher operating frequencies. However, harmonic interference can occur on those frequencies, and, due to this issue, the authors opted to use a lower frequency. The antenna attached on this chip was a 2×2 patch antenna array, fabricated with a RO4003 substrate with $\varepsilon_r = 3.38$ and thickness equal to 0.73 mm. Adjacent patch elements were located with a distance of $0.74\lambda_0$, where λ_0 is the wavelength in free space, in order to decrease side lobes. The developed antenna had a gain equal to 10.77 dBi and HPBW equal to 14.5°.

Later, in [28], a 100 GHz low-IF CW radar transceiver was presented in a 65 nm CMOS chip. In this work, the radar was applied for mechanical vibration and biological vital sign detections. Two horn antennas, operating at 100 GHz, with 20 dBi of gain, were used as TX and RX antennas. Vital signs were acquired, with the subject being seated 2 meters away from the radar. In this case, 65 beats/min were obtained, which agrees with the pulse rate measured using a finger oximeter. In addition, the heart rate of a bullfrog was measured, at 0.6 m away from the radar. These measures were performed under different temperatures—10 °C, 20 °C, 30 °C, and the obtained results were about 22, 41, and 80 beats/min, respectively. In this way, the authors could conclude that, at 100 GHz, the radar was able to detect much smaller chest displacements.

In the same framework of the on-chip embedded alternatives, a microstrip dipole array antenna was developed in [29], to be later integrated along with the radar front-end on the same chip. Dipole antennas have a low profile, are low cost, and they can be arranged in arrays. The authors used a structure with three dipoles disposed symmetrically to obtain a higher gain and used a reflector

to achieve directivity. The proposed antenna operates at 2.4 GHz, within a bandwidth from 2.35 to 2.5 GHz. The main lobe has 10.8 dBi gain, with a beamwidth equal to 49°.

3.4. Mutual Coupling Reduction

Mutual coupling effect occurs when one antenna receives part of the energy radiated from a second antenna located nearby. This can happen due to three main reasons: the radiation pattern of each antenna, the separation between both antennas (which should be at least equal to half wavelength), and the main lobe orientation of both antennas [30]. Furthermore, mutual coupling can alter the radiation pattern of each radiating element, since it shifts the maximum and nulls location, filling the nulls when it was not supposed to [30].

As seen in the previous subsection, when two antennas are used to perform TX and RX, they should be separated sufficiently enough to avoid mutual coupling (generally half wavelength), but the distance between antennas should be enough to guarantee the monostatic radar function. In this sense, the mutual coupling effect must be taken into account, and strategies to decrease its effect should be adopted.

The literature about bio-radar systems that specifies which antennas are being used and their design constraints does not focus on the mutual coupling effect and does not explore different strategies to reduce it. Even though we have seen so far that some authors care about cross-talk and present measures to prove that the TX/RX pair has acceptable levels of coupling. In addition, it is mentioned that the usage of CP approach can be one possible solution for this issue, and it can also enhance other problems inherent to the bio-radar systems.

As we will see in the next subsection, it is possible to use orthogonal polarization in TX and RX because an incident CP wave flips its polarization propagation when reflecting on a surface. Furthermore, if the system uses different rotation directions, such as RHCP for TX and LHCP for RX, there is no power reduction due to the signal rotation when reflecting at the target surface, and there is no mutual interference because, at the front-end stage, antennas have crossed polarization. Thus, a system using CP antennas has low mutual coupling [16].

3.5. Circular Polarization

Linear polarization (LP) is the less complex approach. However, some problems arise with its usage for NCVS applications. After transmitting an LP signal, during propagation, the reflected signal can rotate θ degrees in total, hence the signal at the receiver input has its power decreased by a factor of $\cos\theta$, and the radar sensitivity is largely reduced [17]. Thus, CP is generally the best alternative, since CP antennas are not affected by polarization mismatch. Furthermore, in [31], the authors have pointed out other emerging problems due to the usage of LP antennas. There is fading RCS due to the scattering reflection on the target. The human body is composed of different materials, shapes, sizes, or thickness. Hence, different surfaces cause electric vector rotation, which lead to a misalignment with the receiver antenna. Moreover, the target at hand is moving; consequently, a time-varying RCS arises. CP antennas stable the RCS over time and keep the alignment between scatter signals and the receiver.

In this sense, it is possible to conclude that CP is the best strategy to achieve better SNR and to isolate the system from other radar based systems nearby. In [11], TX and RX antennas with opposite polarization were used, (LHCP for TX and RHCP for RX), in order to isolate the signal reflected by the target from signals derived from other transmitting systems.

The impact of circular polarization in the bio-radar performance was tested in [9]. A set-up was settled with three antennas, where two are for RX and one for TX. Antennas were disposed according to the following scheme: RX1 with RHCP, TX with RHCP and RX2 with LHCP. Antenna TX transmitted a signal towards a metallic reflector, and the signal strength received in RX1 and RX2 were evaluated. The authors observed that the signal at RX2 was 1.2 dB stronger than the signal at RX1 input. This effect can be explained with the isolation of each signal. Thus, it is possible to conclude that the antenna pair TX/RX with opposite polarization is a better option to enhance the SNIR.

More tests were conducted to analyze the effect of the antenna polarization along with beamwidth in the performance of Doppler radar, in [32,33]. Four microstrip patch antennas for bio-radar, operating at 2.4 GHz, were designed and manufactured:

1. LP single patch antenna;
2. CP single patch antenna;
3. 2×2 LP array;
4. 2×2 CP array.

To achieve the same gain for all antennas, different substrates were used to manufacture them, being 1 and 2 printed on RT-Duroid 5880, with $\varepsilon_r = 2.2$ and 1.6 mm thickness, and 3 and 4 made using FR-4, with $\varepsilon_r = 4.4$ and 1.6 mm thickness. In this way, the authors were able to compare only the beamwidth effects on radar performance, excluding the influence of the gain. Sixteen combinations were presented, e.g., CP array used as TX and LP single patch antenna as RX antennas. Five measurements per combination were performed inside an anechoic chamber, during 30 s, using a linear programmable actuator as a moving target. The measured gains of all antennas are within 5.8 dBi. The HPBW is 37° for the array and 81° for the single antennas. All combinations were capable of estimating the motion frequency, and, in summary, the authors concluded that the best radar performance is obtained when they used the antennas 1 and 4 as TX and RX antennas, respectively. In this case, the received signal showed the strongest fundamental frequency amplitude, −6.41 dB. On the other hand, the combination of 4 and 2, used as TX and RX, respectively, showed the worse performance, the fundamental frequency amplitude being equal to −22.77 dB.

By taking advantage of different antenna polarization, in [34], a solution is proposed to mitigate the random body motion using crossed-polarized antennas. Two transceivers are used, one at the back of the subject and other in the front. Since vital signs have the same waveform pattern and periodicity, this system combines both signals and mitigate any waveform that has different pattern and frequency. Since two antennas face each other, their design should be done carefully. In this sense, a 2×2 patch array antenna was used, with vertical polarization for front and horizontal polarization for back transceivers, respectively. The other antennas' parameters are not specified in the paper.

3.6. Customized Antennas for Commercial Transceivers

Some commercially available bio-radars have also been tested. In [35], the authors proposed a new method of blind source separation for signal from multiple subjects. In this work, the authors used a stepped frequency CW bio-radar BioRASCAN-4 (RSLab, Moscow, Russia) [36] that is composed by two horn antennas, operating at 3.6–4.0 GHz, with a constant gain equal to 20 dBi. The combined size of these antennas are $370 \times 150 \times 150$ mm, and it has a 60 dB dynamic range to detect signals. In this experiment, the authors were capable of identifying three different respiratory patterns of the subjects located at the same distance from the radar.

In the same framework of commercial products, a K-LC5 transceiver from RFbeam Microwave GmbH (St. Gallen, Switzerland) [37], operating with 24 GHz carrier, was used in [38] to evaluate if bio-radar technology can be used to access the psychophysiological state of 35 healthy volunteers. In this sense, vital signs were acquired and classified using data-mining techniques and thus determine if there is any mental or physical stress among the subjects. TX and RX antennas of the K-LC5 are patch arrays, which can be used in two different configurations: 3 array, with 80° of HPBW, or 1 array, with 34° of HPBW. The transceiver has a compact size $25 \times 25 \times 6$ mm, and it was designed for short range applications (within 1 m range). The authors on this paper could identify correctly whether the subject was calm or stressed with 80% of accuracy.

In addition, from RFbeam, a K-LC2 transceiver [39] was tested in [40]. The K-LC2 also works at 24 GHz and uses for TX and RX a 2×4 array. The antenna gain is 8.6 dBi and the beamwidth is around 80° and 34° for the E- and H-plane, respectively. In this study, measurements of the vital

signals from a man seated 50 cm away from the radar were done. The developed radar using the K-LC2 transceiver was able to measure 19 beats/min and 64 beats/min, for breathing and heartbeat, respectively, which agrees with the results obtained using a Healthcare HM10 pulse sensor.

3.7. Other Radar Transceivers

In this sub-section, non conventional radar transceivers are approached and the antennas used are described. First, different radar front-ends are seen and front-ends designed to perform beam-steering are mentioned afterwards.

3.7.1. Customized Front-Ends

The research community suggests a varied panoply of solutions to mitigate the inherent problems in the proper detection of vital signs. Solutions vary not only in the antenna design but also in the transceiver hardware. The majority of works presented until now use single hardware components, interconnect and/or integrated on chips which implied analog signal processing. On the other hand, Software Defined Radios (SDR) perform part of the signal processing digitally, which confer more flexibility to the system. In [41], a radar for vital signs measurement using SDR is proposed. Two microstrip patch antenna arrays are used for TX and RX, respectively. Each antenna has eight elements to achieve directivity (8×2 array). The authors underline the advantage of using patch antennas instead of horn antennas which would require a bigger footprint. Antennas are optimized to operate at 5.77 GHz and have a 16 dBi gain. Vital signs were successfully acquired at a distance of 0.5 m.

Some other solutions were presented to adapt the transceiver operational mode to environment issues. For example, the motions of the proper radar handling were considered in [42] as a noise source and a possible solution was presented. The system proposed by the authors uses a Doppler radar that transmits a fundamental signal component at 2.4 GHz towards the target, and simultaneously transmits a harmonic signal component at 4.8 GHz towards a stationary reflector, located on the opposite side. This system receives the reflected signal from the main target, as well as the signal reflected by the reflector. Both signals are phase modulated due to the chest-wall motion and the radar handling motion, respectively. Thus, it is possible to remove the noise caused by radar handling, through self-cancellation implementation.

The antennas used in this set-up had a gain equal to 8 dBi approximately and a HPBW equal to 80° for the fundamental antennas and 70° for the harmonic antenna. Since two pairs of antennas are located back to each other, a high front-to-back ratio was required and it was accomplished, being better than 21 dB. The coupling between antennas was -32 dB for the fundamental antenna pair and -40 dB for the harmonic antenna pair.

In [43], a radar system for NCVS was prepared using standard equipment that can be found in any RF laboratory. In this way, some inherent problems are immediately solved, such as the DC component offset calibration or the In-phase and Quadrature (IQ) imbalance, and thus a bio-radar prototype can be rapidly built for research purposes, without caring with possible hardware problems that can come along with portable transceivers. With this set-up, it was possible to retune the system for different carrier frequencies and monitor multiple targets. The authors have captured vital signs using two different antennas, in order to evaluate the system's performance for single-frequency operation mode, for frequency-tuning experiments, and for capturing vital signs with objects in front of the target. The first antenna was a 2×2 microstrip patch array, operating at 2.4 GHz. Two equal antennas were fabricated together, where one was used for TX and the other for RX. The FR-4 substrate was used, with $\varepsilon_r = 4.6$ and thickness equal to 1.5 mm. The final size of dual-incorporated antennas was 459×222 mm, and it was measured in an anechoic chamber. It had as a maximum gain 6.5 dBi and as HPBW 40°. The second antenna, was a commercial horn antenna (HD-10180DRHA, Hengda Microwave, Xi'an, China), with broadband between 1 GHz to 18 GHz. The gain of this antenna varied according to the frequency, between 10 and 16.5 dBi.

The experiments were carried out successfully for all three test scenarios. With single-frequency operation mode, vital signs were acquired accurately, as compared with reference measurements. On the other hand, for variable frequency carriers, the results were not always accurate. With fixed transmitted power, the amplitude of vital signs decreased for the higher frequency component (18 GHz), due to cable attenuation, antenna coupling, and free-space attenuation. Finally, the obstacles experiment was conducted with the fixed 2.4 GHz frequency and vital signs were measured accurately.

3.7.2. Beam-Steering Systems

Many problems can arise when detecting vital signs in moving subjects. As seen previously, the human chest-wall has a small RCS, which has a limited area around 0.5 m^2, and the proper alignment should be guaranteed to acquire signals with optimal SNR. Fixed-beam antennas require this alignment for every different subject, since humans have different heights and body structures. In this framework, beam-steering technology can be advantageous since it can re-direct the beam seeking for the best SNR.

In [44], an adaptive beam-steering antenna is proposed, in order to increase the detectable range without increase the system size. A 2×2 microstrip patch antenna array and two phase shifters are embedded on the same board. The developed antenna has 200 MHz of bandwidth, centered in 5.8 GHz and it can steer from -22° to 22° within the H-plane. Phase array antennas can steer to different angles if the adjacent antennas are fed with different phased signals, by using phase shifters [44]. Antennas are built using a Rogers4350B substrate. The S_{11} values were far below -10 dB for all steering angles, from -22° to 22°. The HPBW was equal to 41°, which leads to total coverage of 85°.

To test the performance of a system with a beam-steering approach, a subject located at the angle of 21.8° was monitored using both fixed-beam and beam-steering antennas. By using beam-steering antennas, several angles were scanned. The cardiac signal was detected with the beam-steering antenna at the angle where the subject was located and the remain angles, as well as the fixed-beam antenna, presented only noise.

A NCVS system was designed for multi-target monitoring in [45]. For this purpose, a phased-array CW radar, operating at 2.4 GHz was developed to generate two different beams concurrently. Thus, it was possible to capture respiratory signals from two subjects at the same time using the same carrier. To perform the phased-array radar, two linear arrays were used with four elements each, for both TX and RX. Single elements were rectangular patches, spaced 8 cm between each other. Measurements of antennas were performed inside and outside of the anechoic chamber, to verify the impact of propagation environment on its radiation pattern. For both cases, it was possible to obtain good agreement between simulated and measured radiation patterns. Furthermore, as expected, the side-lobe level increased on measurements outside the anechoic chamber since there are other systems operating at the same frequency. Dual-beam mode was also measured under the same conditions. Two situations were considered: in the first case, one beam was directed to -15° and the other directed to 25°, while the second situation had one beam directed to -25° and the other directed to 30°. Results were similar for main lobes, for both simulation and measurement cases, but had slightly differences respecting the sidelobes that were justified due to some minor errors in circuits and cables.

Metamaterials were explored in the NCVS radar systems, in [46]. In this work, metamaterial-based scanning leaky-wave antenna is developed for beam-scanning Doppler radar, with the steering angles between -33° and 26°. This system can track the human subject and measure vital signs. The main beam is frequency controlled, which means that the system should be retuned within the frequency range of 5.1–6.5 GHz in order to be able to scan all steering angles.

The antenna was fabricated using two layers of FR-4 substrate, with $\varepsilon_r = 4.4$, loss tangent of 0.02 and with thickness equal to 0.2 mm and 1.23 mm, respectively. The antenna is composed by 30-cells (where one cell corresponds to a single element), disposed linearly. Antenna gains varied with the frequency, being 5 dBi for 5.1 GHz, 7.1 dBi for 5.8 GHz and 6.8 dBi for 6.5 GHz.

With this set-up, it was possible to detect two subjects located at 0° and 26° angles, respectively; thus, frequencies of 5.8 GHz and 6.5 GHz were the ones being used. Their vital signs were successfully measured.

4. Antennas for UWB Operation Mode

Similarly to the previous section, herein it is presented antenna design examples, considering the UWB operation mode for NCVS applications. UWB radars have a different working principal, which requires high operation bandwidth. Therefore, the antenna design should be suitable for this purpose.

4.1. General Antenna Considerations for UWB Systems

Different antennas were evaluated and compared in [47]. An experiment was made, where the respiratory signal was acquired using three antennas with different designs, as described in Table 1. Thus, different characteristics concerning the radiation pattern, gain and cross-polarization were tested. Their set-up was composed by a UWB radar operating within the bandwidth 3.1 GHz–5.3 GHz.

Table 1. Antennas tested and compared in [47].

Antenna Design	Radiation Pattern	Gain	Bandwidth (GHz)
Broadspec UWB antenna	Omnidirectional	low gain	3.4–10.4
Horn antenna	Directive	high gain	2–18
Doubled layered Vivaldi antenna	Directive	medium gain	3.3–10

The best results were achieved with the Vivaldi antenna, which has a medium gain, a directive radiation pattern, and the best co- and cross-polarization ratio. The remaining antennas had the worst performance, due to different aspects. First, the omnidirectional antenna transmits the same power in every direction, which means that unwanted reflections are equally received as the wanted ones. This antenna also had the worst co- and cross-polarization ratio, which means high cross-polarization components. Then, the horn antenna has bigger dimensions and its radiation pattern is highly directive. This obliges a perfect alignment between the target and both TX and RX antennas that have be separated. This balance is difficult to achieve.

Moreover, UWB antennas are known to have dispersive behavior, i.e., radiate in different frequency components. This occurs due to a phase center instability, as stated in [48]. The phase center deviation can cause signal distortion and can contribute to the error on respiratory rate computation. Phase center deviations were highly perceived for the Broadspec UWB and horn antenna and were less evident for Vivaldi antenna.

The performance was evaluated after the respiratory rate error computation, considering a reference rate. Several experiments were performed, where different set-up parameters varied, such as the target motion frequency (to imitate the respiratory rate), the motion amplitude, and the nominal distance between the radar and the target. It is important to note that all the error rates had increased with this latter parameter, but the error was more significant for the Broadspec UWB and Horn antennas rather than Vivaldi antenna.

4.2. Antenna Performance Improvement

The characteristics for an acceptable UWB antenna were identified in the previous sub-section: directional radiation pattern, high gain, compact size, good co- and cross-polarization ratio, and non-existence of phase center deviations. Nevertheless, antenna features should be optimized for each application, and some techniques applied for this purpose are described in this sub-section.

4.2.1. Gain and Bandwidth

Different techniques to improve the gain and broadband characteristics were developed in [49]. They used a partial ground plane patch to achieve wideband coverage (4.3 GHz to 7 GHz), combined with parasitic patches emulating the Yagi concept, to improve gain. In the end, the authors also compared the performance of the final antenna with a single-patch with a partial ground plane as well. It was possible to conclude that single-patch is worse than the proposed one since it does not have sufficient gain, has a wide beam (hence, has lack of directivity) and it does not confer enough isolation when two antennas are side by side.

Furthermore, the antenna developed in [49] was also focused on indoor applications considering a specific location inside a room. The presented layout encompassed a ground plane working as a reflector and parasitic patches working as directors. The beam angle was designed to allow the antenna to be located on the ceiling, in the corner of a room. For this purpose, the main lobe was directed to a specific angle (35°), through a mutual coupling effect. Regarding the radiation pattern, the HPBW was equal to 43°.

In [50], another antenna for indoor applications is proposed. A Ground Surround Antenna (GSA) array was designed, considering the framework of NCVS acquisition. The development of antennas for indoor applications should meet some beamwidth and range requirements, in order to mitigate multipath interferences that can occur due to reflections on walls or furniture. In this sense, the authors state that the beamwidth should be no larger than 30° and the gain can be improved by applying a superstrate layer. The GSA also has higher bandwidth rather than a conventional patch. Thus, the antenna array developed in [50] had a maximum gain equal to 12.2 dBi, an HPBW of 26° and bandwidth within 2.28 GHz–2.49 GHz, centered at 2.45 GHz.

4.2.2. Polarization

Within general performance characteristics, the advantages of CP were explored for the UWB radar in [31]. The Axial Ratio (AR) of the developed antenna is preserved in all bandwidths, by using an array of LP antennas arranged in a sequential rotation manner, with 90° rotations. The selected antenna design is a dual elliptically tapered antipodal slot and two different sequential arrangements were considered: a 'box' and a 'cross' arrangement. Antennas were fabricated using a Rogers 4003C substrate and with a total size of 9×9 cm^2. The LHCP was the selected polarization since it has less interference from the existent wireless equipment, which is operating in the same band. They proved the robustness of the system using CP antennas by comparing the amplitude of the received signal with four different polarization angles and the wave amplitude remained approximately the same. Furthermore, the accuracy on detecting the heartbeat was 2 beats/min superior rather than using LP antennas.

4.3. Antennas Customization for Different UWB Radar Applications

Many radar applications were presented in the literature with a UWB front-end. For example, in [51], the authors use a UWB bio-radar, with impulse radios, to monitor multiple human targets. The proposed system consists of one TX and three RX antennas, to form three independent channels. All antennas are bow-tie dipoles working at centered frequency 500 MHz and with equal bandwidth. The antennas were tested in four different scenarios: with no target, single target, and two and three targets behind a brick wall with 28 cm of thickness. The results have shown that, besides the acquired respiration waveform being quite different, depending on the channel, in all cases, the UWB radar was able to detect the respiration patterns of the human targets.

Then, a non-contact system to acquire vital signs were presented in [52], with a different operation mode. Instead of using a Doppler radar, the respiratory rate is evaluated through phase differences in the S_{11} coefficient. For this purpose, they combine the UWB with CW principles to take advantage of both techniques. Nonetheless, their concern about antenna characteristics is the same. The goal

of their work is to develop an antenna with small size, low cost, with directional radiation pattern, large bandwidth, and good impedance matching over all bands. The front-to-back lobe ratio was also a concern to reduce the possible interference from parasitic reflections in objects within the antenna's range.

To fulfill all these requirements, a microstrip slot antenna was developed to operate within 3 GHz to 5 GHz bandwidth. A circular patch was used to cover this bandwidth with an acceptable match impedance, and a reflector plane was added behind the ground plane, to provide a directive beam. Finally, a metallic box was used in the antenna and reflector surroundings, to isolate the antenna from adjacent reflections, and thus improve the front-to-back lobe ratio. The metallic box also helps to narrow the radiation pattern. In the end, the final antenna presented the following characteristics, at the central frequency of 4 GHz: HPBW equal to 46°, gain equal to 9.3 dBi, and S_{11} coefficient between −20 and −10 dB within all bandwidths.

5. Discussion

As several antennas have been reported throughout this manuscript, for a better overview, Table 2 summarizes some characteristics of the antennas that were developed for bio-radar applications.

Table 2. Summary of the parameters of the reviewed antennas.

Radar Mode	Ref.	Antenna Type	Central Frequency (GHz)	Bandwidth (GHz)	Gain (dBi)	HPBW
CW	[9]	Axial-mode helical antenna	2.4	-	9.80	44.6°
		Patch antenna	2.4	-	-	60°
	[10]	One-dimensional patch array	24	-	8	33.7°
	[12]	Microstrip patch array (8 × 2)	24	24–25	17.15	-
		Microstrip patch array (8 × 6)	24	23.3–23.7	17	-
	[13]	Microstrip patch array (10 × 16)	77	74.6–79.7	25	12°
	[14]	SIW slot array	12	-	13	-
		SIW slot array	24	-	24	-
	[15]	Fractal-slot patch antenna	0.915	0.907–0.924	5.8	108°
	[18]	Yagi patch antenna	2.45	-	8.69	-
	[19]	Horn antenna	-	50–75	25	7°
	[20]	Annular ring patch antenna	2.4	-	-	132°
	[22]	Microstrip patch array	10	-	8	30°
	[23]	Microstrip patch array (2 × 1)	60	57.24–65.88	13	-
		Microstrip patch array (3 × 3)	60	57.24–65.88	16	-
		Microstrip patch array (6 × 2)	60	57.24–65.88	16	-
	[25]	Microstrip patch array (4 × 5)	24	-	17	24°
	[26]	Printed patch array (2 × 2)	5	-	9.7	20°
	[27]	Patch array attached to CMOS chip	5.8	-	10.77	14.5°
	[29]	Dipole array	2.4	2.53–2.4	10.8	49°
	[32]	Microstrip patch antenna	2.4	-	5.8	81°
		Microstrip patch array	2.4	-	5.8	37°
	[35]	Horn antenna	-	3.6–4	20	-
	[38]	Three Patch array	24	-	8.6	80°
		Single patch array	24	-	8.6	34°
	[40]	Microstrip patch array (2 × 4)	24	-	8.6	80°
	[41]	Microstrip patch array	5.77	-	16	-
	[42]	Aperture-coupled patch antenna	2.4	-	8	80°
		Aperture-coupled patch antenna	4.8	-	8	70°
	[43]	Microstrip patch array (2 × 2)	2.4	-	6.5	40°
	[44]	Adaptive beam-steering antenna	5.8	5.7–5.9	-	41°
UWB	[49]	Partial ground plane combined with parasitic patches emulating Yagi concept	4.37	4.3–7	-	43°
	[50]	GSA array	2.45	2.28–2.49	12.2	26°
	[52]	Microstrip slot antenna	4	3–5	9.4	46°

As one can see in Table 2, several designs have been proposed for different bio-radar application scenarios. Planar patch antennas were the type of antennas most used in the reviewed papers. This preference can be explained by the fact that this type of antenna has a low cost, low profile, is easy to be fabricated, and can potentially be integrated with the radar circuitry on the same printed circuit board.

Observing the characteristics of the revised antennas, the most used frequencies are 2.4 GHz, 5.8 GHz, 24 GHz, and 60 GHz, and typically the antennas presented a narrow bandwidth. In addition, the gains can vary between 5.8–25 dBi. Generally, the arrays show higher gain (10.8–25 dBi), when compared with a single antenna (5.8–9.80 dBi). As an exception, the single horn antennas presented in [19,35] had gain equal to 25 dBi and 20 dBi, respectively.

Regarding the materials used for the development of antennas for bio-radar, it seems to be a preference to commercial available low-cost materials, with well-known electromagnetic characteristics. Table 3 summarizes the materials used as a dielectric substrate in the reviewed antennas.

Table 3. Summary of the materials used as a dielectric substrate for bio-radar antennas.

Ref.	Antenna Frequency (GHz)	Substrate	ε_r
[18]	2.45	RF-4	4.4
[34]	2.4		
[24]	0.9–12		
[15]	0.9–2.5		
[12]	24	FR-4	3.55
[23]	60	Duroid	2.2
[25]	24	RO4350	3.48
[32]	2.4	RT-Duroid5880	2.2
[27]	5.8	RO4030	3.38
[10]	24.125	RO4835	3.66
[13]	77	RO3003C	3.0

Although the commercially available substrate materials had the permittivity values very well characterized by the manufacturer, some attention has to be taken during the design of ultra-wideband antennas. In this case, as reported before, the use of a single permittivity value during the simulation process for all bands can influence the results of the antenna in different frequencies.

After analyzing all the examples and the most common choices, some trade-offs can be established for the optimal antenna design, considering NCVS applications.

Starting with the signal quality matter, larger antennas confer directive beams, but antennas with larger sizes also have a larger near-field region [5], where the electromagnetic propagation can not be modelled linearly. In these cases, there is more area where the antenna behavior can not be foreseen. Nonetheless, directivity is seen by many authors as a crucial characteristic to accomplish high SNR and accuracy in NCVS signals, since it reduces the parasitic reflections and decreases clutter interference. In parallel, the main lobe beamwidth should not be too narrow, since, subsequently, a perfect alignment with the subject's chest-wall would be required. These also hamper the generalization of system operation by extending it to multiple subjects, since humans have different body structures and heights and prior calibrations would be needed.

The system size is also a concern, to enable its portability and to facilitate its usage. Using a single antenna for both TX and RX operations could be an immediate solution. However, proper isolation must be assured where the selection of low cost and simpler hardware components is preferable. Opting by two separate antennas implies that antennas should be closed together, so the radar operation is approximately as a monostatic, and the RCS is preserved [5]. Either way, i.e., using a single antenna or two separate antennas, the cross-talk must be minimized.

Regarding the frequency of operation, it is directly related to the radar operation mode, even though there are some studies that aim to determine the optimal frequency band for NCVS

applications. In [53], a mathematical model and its simulation are presented to seek for the best operating frequency that allows both respiratory signal and cardiac detection. They conclude that the signal strength increases when using frequencies above 5 GHz, and it stabilizes until the lower region of the K-band. Above 20 GHz, the signal strength decreases slightly. Moreover, nonlinear phase modulation causes harmonic intermodulation, which is more evident for frequencies above 27 GHz than for frequencies around 5 GHz.

In [53], the authors also studied the relation between frequency and beamwidth. They considered large beamwidth above 20° of HPBW and narrow beamwidth around 7°. It was possible to conclude that signal strength from heartbeat and respiration varies with the frequency, if a large beamwidth is used. On the other hand, the signal strength is stable for narrow beamwidths. Hereinafter, the gain range for bio-radar applications was proposed in [29], where the authors state that a gain under 5 dBi is not enough, and the typical gain value for antennas applied in NCVS acquisition is around 9 dBi.

In summary, some key features directly influence the quality of the signal acquisition and take action in the system manufacturing. Figures 2 and 3 present the main characteristics that the authors took into account, when developing antennas for bio-radar applications.

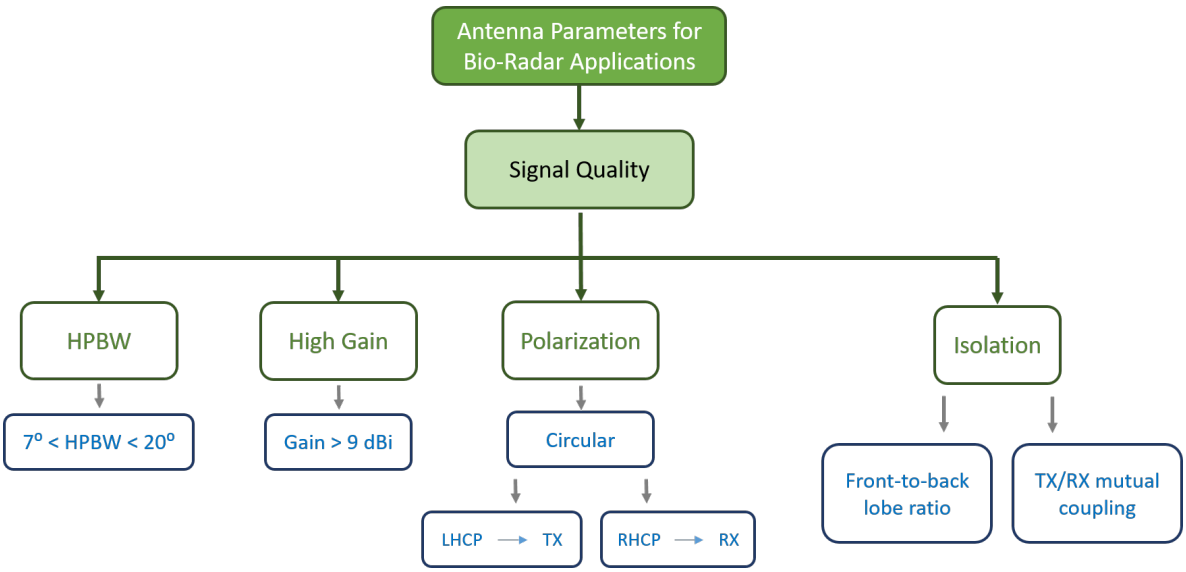

Figure 2. Antenna parameters to improve the acquired signal quality.

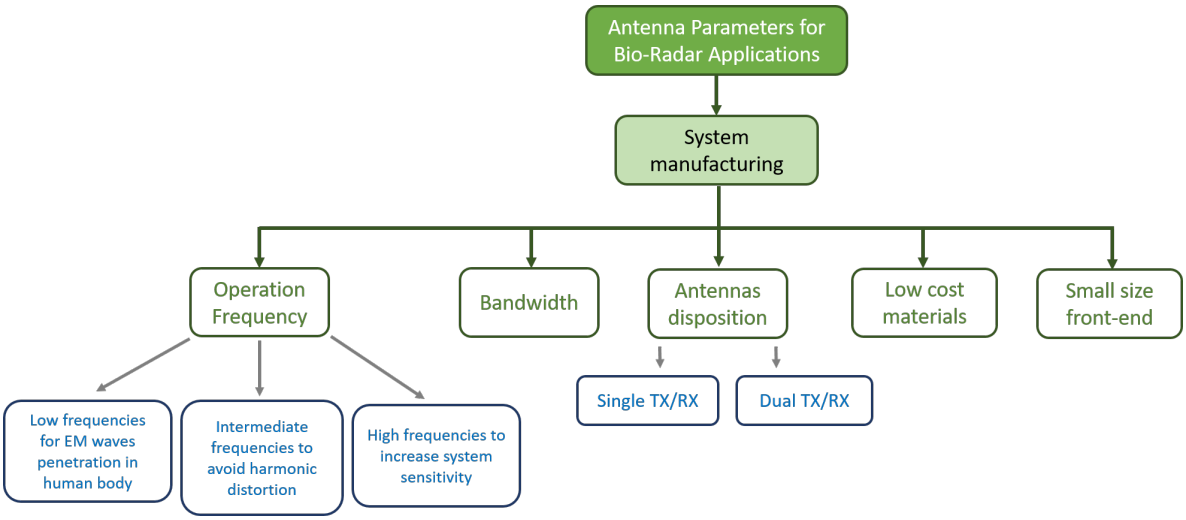

Figure 3. Antenna parameters to consider for manufacturing purposes.

6. Conclusions

With the advance of wireless technologies, remote health monitoring has become an emerging solution to promote well-being and to detect emergencies at indoor and outdoor scenarios.

In this way, several studies using Doppler radar for NCVS have been presented in the past years. However, most of them have described the development and/or improvement of the radar circuit based on demodulation methods and algorithms. As the antenna is a crucial part of the NCVS systems, a gap of information regarding the antennas parameters suitable for bio-radar was identified.

The knowledge of the effects of the antenna characteristics can help to improve the performance of radar systems, such as detection accuracy and sensitivity. Throughout this work, several solutions to improve signal acquisition were described. In summary, there is not a single solution to enhance antenna performance. Despite that, based on the presented survey, some guidelines for the design of antennas for vital signs acquisition using radar technology, are pointed out:

- Frequencies—High frequencies increase the sensibility of the radar system and intermediate frequencies can avoid harmonic distortion. Furthermore, low frequencies can be applied for surveillance and finding people applications due to the good penetration capacity of the EM wave through the materials.
- Circular polarization, with different rotation direction in TX and RX, is preferable—using different rotation direction increases the isolation between the transmitter and the receiver, minimizing negative influences of second order reflections and multi patch effects on the system;
- Avoid circulator usage if a single antenna is used. Instead, use alternative hardware components for signals division that do not decrease signal power;
- Directivity—directive beams can achieve high SNR and accuracy in NCVS signals, since its reduces parasitic reflections and decreases clutter interference;
- High gain—above 9 dBi at the main lobe is preferable. An array can be used to achieve a higher gain instead of a single antenna;
- Reduced size of the antennas can improve the portability of the system;
- The use of low cost materials.

Author Contributions: All the authors have contributed to this paper. C.G. and C.L. did the full research, its discussion, and wrote the manuscript. P.P. and J.V. did the technical revision of this manuscript and supervised all the research work.

Funding: This work is funded by National Portuguese Funds through FCT—Fundação para a Ciência e Tecnologia under the PhD grant SFRH/BD/139847/2018. The work also is supported by FCT/MEC through national funds and when applicable co-funded by European Regional Development Fund (FEDER) PT2020 in partnership agreement under the project UID/EEA/50008/2018 and UID/Multi/00195/2018; and by the FEDER, through the Competitiveness and Internationalization Operational Program (COMPETE 2020) of the PT2020 framework [Mobilizing Project TexBoost, under the Postdoctoral grant 024523-PPS4-AN1].

Conflicts of Interest: The authors declare no conflict of interest.

Abbreviations

The following abbreviations are used in this manuscript:

AR	Axial Ratio
CMOS	Complementary Metal-Oxide-Semiconductor
CP	Circular Polarization
CW	Continuous Wave
EM	Electromagnetic
FMCW	Frequency-Modulated Continuous Wave
GSA	Ground Surround Antenna
HPBW	Half-Power Beamwidth
IQ	In-phase and Quadrature
LHCP	Left-Hand Circular Polarization

LNA	Low Noise Amplifier
LP	Linear Polarization
LTCC	Low-Temperature Co-Fired Ceramic
NCVS	Non-contact Vital Signs
PCB	Printed Board Circuit
QHC	Quadrature Hybrid Coupler
RCS	Radar-Cross Section
RF	Radio-Frequency
RHCP	Right-Hand Circular Polarization
RX	Reception
SDR	Software Defined Radio
SIW	Substrate Integrated Waveguide
SNR	Signal-to-Noise Ratio
SNIR	Signal-to-Noise-plus-Interference Ratio
TX	Transmission
UWB	Ultra-Wide Band

References

1. Mpanda, R.S.; Liang, Q.; Xu, L.; Lin, Q.; Shi, J. Investigation on Various antenna design techniques for Vital Signs Monitoring. In Proceedings of the Cross Strait Quad-Regional Radio Science and Wireless Technology Conference (CSQRWC), Xuzhou, China, 21–24 July 2018. [CrossRef]
2. Gouveia, C.; Malafaia, D.; Vieira, J.N.; Pinho, P. Bio-radar performance evaluation for different antenna designs. *URSI Radio Sci. Bull.* **2018**, *364*, 30–38.
3. Boric-Lubecke, O.; Lubecke, V.M.; Droitcour, A.D.; Park, B.-K.; Singh, A. *Doppler Radar Physiological Sensing*; John Wiley & Sons: Cambridge, UK, 2015.
4. Skolnik, M.I. *Introduction to Radar Systems*; Mc Grow-Hill: New York, NY, USA, 2001.
5. Droitcour, A.D. Non-Contact Measurement of Heart and Respiration Rates with a Single-Chip Microwave Doppler Radar. Ph.D. Thesis, Stanford University, Stanford, CA, USA, 2006.
6. Taylor, J.D. *Ultra-Wideband Radar Technology*; CRC Press: Boca Raton, FL, USA, 2000.
7. Das, V.; Boothby, A.; Hwang, R.; Nguyen, T.; Lopez, J.; Lie, D.Y.C. Antenna evaluation of a non-contact vital signs sensor for continuous heart and respiration rate monitoring. In Proceedings of the IEEE Topical Conference on Biomedical Wireless Technologies, Networks, and Sensing Systems (BioWireleSS), Santa Clara, CA, USA, 15–18 January 2012; pp. 13–16.
8. Fletcher, R.; Han, J. Low-cost differential front-end for Doppler radar vital sign monitoring. In Proceedings of the IEEE MTT-S International Microwave Symposium Digest, Boston, MA, USA, 7–12 June 2009; pp. 1325–1328.
9. Boothby, A.; Hwang, R.; Das, V.; Lopez, J.; Lie, D.Y.C. Design of Axial-mode Helical Antennas for Doppler-based continuous non-contact vital signs monitoring sensors. In Proceedings of the IEEE Radio and Wireless Symposium, Santa Clara, CA, USA, 15–18 January 2012; pp. 87–90.
10. Schäfer, S.; Diewald, A.R.; Schmiech, D.; Müller, S. One-dimensional Patch Array for Microwave-based Vital Sign Monitoring of Elderly People. In Proceedings of the 19th International Radar Symposium (IRS), Bonn, Germany, 20–22 June 2018; pp. 1–10.
11. Shen, T.; Kao, T.J.; Huang, T.; Tu, J.; Lin, J.; Wu, R. Antenna Design of 60-GHz Micro-Radar System-In-Package for Noncontact Vital Sign Detection. *IEEE Antennas Wirel. Propag. Lett.* **2012**, *11*, 1702–1705. [CrossRef]
12. Lan, S.; Xu, Y.; Chu, H.; Qiu, J.; He, Z.; Denisov, A. A Novel 24 GHz Microstrip Array Module Design for Bioradars. In Proceedings of the International Symposium on Antennas and Propagation (ISAP), Hobart, Australia, 9–12 November 2015; pp. 1–3.
13. Lan, S.; Duan, L.; He, Z.; Yang, C.; Denisov, A.; Ivashov, S.; Anishchenko, L. A 77 GHz Bioradar Antenna Module Design Using Microstrip Arrays. In Proceedings of the IEEE International Symposium on Antennas and Propagation (APSURSI), Fajardo, Puerto Rico, 26 June–1 July 2016; pp. 1177–1178.

14. Chioukh, L.; Boutayeb, H.; Deslandes, D.; Wu, K. Noise and sensitivity analysis of harmonic radar system for vital sign detection. In Proceedings of the IEEE MTT-S International Microwave Workshop Series on RF and Wireless Technologies for Biomedical and Healthcare Applications (IMWS-BIO), Singapore, 9–11 December 2013; pp. 1–3.
15. Park, J.-H.; Jeong, Y.-J.; Lee, G.-E.; Oh, J.-T.; Yang, J.-R. 915-MHz Continuous-Wave Doppler Radar Sensor for Detection of Vital Signs. *Electronics* **2019**, *8*, 855. [CrossRef]
16. Gu, C.; He, Y.; Zhu, J. Noncontact Vital Sensing With a Miniaturized 2.4 GHz Circularly Polarized Doppler Radar. *IEEE Sens. Lett.* **2019**, *3*, 1–4. [CrossRef]
17. Kim, J.-G.; Sim, S.-H.; Cheon, S.; Hong, S. 24 GHz circularly polarized Doppler radar with a single antenna. In Proceedings of the European Microwave Conference, Paris, France, 25–27 October 2005; pp. 1382–1386.
18. Bo, H.; Fu, Q.; Xu, L.; Lure, F.; Dou, Y. Design and implementation of a 2.45 GHz RF sensor for non-contacting monitoring vital signs. In Proceedings of the Computing in Cardiology Conference (CinC), Vancouver, BC, Canada, 11–14 September 2016; pp. 1113–1116.
19. Chuang, H.; Kuo, H.; Lin, F.; Huang, T.; Kuo, C.; Ou, Y. 60-GHz Millimeter-Wave Life Detection System (MLDS) for Noncontact Human Vital-Signal Monitoring. *IEEE Sens. J.* **2012**, *12*, 602–609. [CrossRef]
20. Myoung, S.-S.; Park, J.-H.; Yook, J.-G.; Jang, B.-J. 2.4 GHz Bio-radar System with Improved Performance by Using Phase-Locked Loop. *Microw. Opt. Technol. Lett.* **2010**, *52*, 2074–2076. [CrossRef]
21. An, Y.-J.; Hong, Y.-P.; Jang, B.-J.; Yook, J.-G. Comparative Study of 2.4 GHz and 10 GHz Vital Signal Sensing Doppler Radars. In Proceedings of the 40th European Microwave Conference, Paris, France, 28–30 September 2010; pp. 501–504.
22. Myoung, S.-S.; An, Y.-H.; Yook, J.-G.; Jang, B.-J.; Moon, J.-H. A Novel 10 GHz Super-Heterodyne Bio-Radar System Based on a Frequency Multiplier and Phase-Locked Loop. *Prog. Electromagn. Res. C* **2010**, *19*, 149–162. [CrossRef]
23. Rabbani, M.S.; Ghafouri-Shiraz, H. Ultra-Wide Patch Antenna Array Design at 60 GHz Band for Remote Vital Sign Monitoring with Doppler Radar Principle. *J. Infrared Millim. Terahertz Waves* **2017**, *38*, 548–566. [CrossRef]
24. Van, N.T.P.; Tang, L.; Minh, N.D.; Hasan, F.; Mukhopadhyay, S. Extra Wide Band 3D Patch Antennae System Design for Remote Vital Sign Doppler Radar Sensor Detection. In Proceedings of the Eleventh International conference on Sensing Technology (ICST), Sydney, Australia, 4–6 December 2017; pp. 1–5.
25. Hsu, T.W.; Tseng, A.C.H. Compact 24 GHz Doppler Radar Module for Non-Contact Human Vital Sign Detection. In Proceedings of the International Symposium on Antennas and Propagation, Okinawa, Japan, 24–28 October 2016; pp. 994–995.
26. Xiao, Y.; Li, C.; Lin, J. A Portable Noncontact Heartbeat and Respiration Monitoring System Using 5-GHz Radar. *IEEE Sens. J.* **2007**, *7*, 1042–1043. [CrossRef]
27. Huang, J.; Tseng, C. A 5.8-GHz radar sensor chip in 0.18-µm CMOS for non-contact vital sign detection. In Proceedings of the IEEE International Symposium on Radio-Frequency Integration Technology (RFIT), Taipei, Taiwan, 24–26 August 2016; pp. 1–3.
28. Ma, X.; Wang, Y.; Song, W.; You, W.; Lin, J.; Li, L. A 100-GHz Double-Sideband Low-IF CW Doppler Radar in 65-CMOS for Mechanical Vibration and Biological Vital Sign Detections. In Proceedings of the IEEE MTT-S International Microwave Symposium, Boston, MA, USA, 2–7 June 2019; pp. 136–139.
29. Liang, Q.; Mpanda, R.S.; Wang, X.; Shi, J.; Xu, L. A Printed Dipole Array Antenna for Non-contact Monitoring System. In Proceedings of the Cross Strait Quad-Regional Radio Science and Wireless Technology Conference (CSQRWC), Xuzhou, China, 21–24 July 2018. [CrossRef]
30. Balanis, C.A. *Antenna Theory: Analysis and Design*, 4th ed.; John Wiley & Sons: Hoboken, NJ, USA, 2016; pp. 474–953.
31. Chan, K.K.; Tan, A.E.; Rambabu, K. Circularly Polarized Ultra-Wideband Radar System for Vital Signs Monitoring. *IEEE Trans. Microw. Theory Tech.* **2013**, *61*, 2069–2075. [CrossRef]
32. Nosrati, M.; Tavassolian, N. Experimental Study of Antenna Characteristic Effects on Doppler Radar Performance. In Proceedings of the IEEE International Symposium on Antennas and Propagation & USNC/URSI National Radio Science Meeting, San Diego, CA, USA, 9–14 July 2017; pp. 209–211.

33. Nosrati, M.; Tavassolian, N. Effects of Antenna Characteristics on the Performance of Heart Rate Monitoring Radar Systems. *IEEE Trans. Antennas Propag.* **2017**, *65*, 3296–3301. [CrossRef]
34. Li, C.; Lin, J. Complex signal demodulation and random body movement cancellation techniques for non-contact vital sign detection. In Proceedings of the IEEE MTT-S International Microwave Symposium Digest, Atlanta, GA, USA, 15–20 June 2008; pp. 567–570.
35. Anishchenko, A.; Razevig, V.; Chizh, M. Blind Separation of Several Biological Objects Respiration Patterns by Means of a Step-Frequency Continuous-Wave Bioradar. In Proceedings of the IEEE International Conference on Microwaves, Antennas, Communications and Electronic Systems (COMCAS), Tel-Aviv, Israel, 13–15 November 2017; pp. 1–4.
36. Remote Sensing Laboratory; Bauman Moscow State Technical University. BioRASCAN Radar for Detection and Diagnostic Monitoring of Humans. Available online: http://www.rslab.ru/english/product/biorascan/ (accessed on 30 September 2019).
37. RFBeam. K-LC5 High Sensitivity Dual-Channel Transceiver. Available online: https://www.rfbeam.ch/product?id=9 (accessed on 30 September 2019).
38. Anishchenko, L. Challenges and Potential Solutions of Psychophysiological State Monitoring with Bioradar Technology. *Diagnostics* **2018**, *8*, 73. [CrossRef] [PubMed]
39. RFBeam. K-LC2 Dual Channel Radar Transceiver. Available online: https://www.rfbeam.ch/product?id=5 (accessed on 28 October 2019).
40. Li, P.; Hou, N. A Portable 24 GHz Doppler Radar System for Distant Human Vital Sign Monitoring. In Proceedings of the 5th International Conference on Information Science and Control Engineering, Zhengzhou, China, 20–22 July 2018; pp. 1050–1052.
41. Malafaia, D.; Oliveira, B.; Ferreira, P.; Varum, T.; Vieira, J.; Tomé, A. Cognitive bio-radar: The natural evolution of bio-signals measurement. *J. Med. Syst.* **2016**, *40*, 219. [CrossRef] [PubMed]
42. Zhu, F.; Wang, K.; Wu, K. A Fundamental-and-Harmonic Dual-Frequency Doppler Radar System for Vital Signs Detection Enabling Radar Movement Self-Cancellation. *IEEE Trans. Microw. Theory Tech.* **2018**, *66*, 5106–5118. [CrossRef]
43. Gu, C.; Li, C.; Lin, J.; Long, J.; Huangfu, J.; Ran, L. Instrument-Based Noncontact Doppler Radar Vital Sign Detection System Using Heterodyne Digital Quadrature Demodulation Architecture. *IEEE Trans. Instrum. Meas.* **2010**, *59*, 1580–1588.
44. Nieh, C.; Lin, J. Adaptive beam-steering antenna for improved coverage of non-contact vital sign radar detection. In Proceedings of the IEEE MTT-S International Microwave Symposium (IMS2014), Tampa, FL, USA, 1–6 June 2014; pp. 1–3.
45. Nosrati, M.; Shahsavari, S.; Lee, S.; Wang, H.; Tavassolian, N. A Concurrent Dual-Beam Phased-Array Doppler Radar Using MIMO Beamforming Techniques for Short-Range Vital-Signs Monitoring. *IEEE Trans. Antennas Propag.* **2019**, *67*, 2390–2404. [CrossRef]
46. Tseng, C.-H.; Chao, C.-H. Noncontact vital-sign radar sensor using metamaterial-based scanning leaky-wave antenna. In Proceedings of the IEEE MTT-S International Microwave Symposium (IMS), San Francisco, CA, USA, 22–27 May 2016; pp. 1–3.
47. Alemaryeen, A.; Noghanian, S.; Fazel-Rezai, R. Antenna Effects on Respiratory Rate Measurement Using a UWB Radar System. *IEEE J. Electromagn. RF Microw. Med. Biol.* **2018**, *2*, 87–93. [CrossRef]
48. Schantz, H.G. Introduction to Ultra-wideband Antennas. In Proceedings of the IEEE Conference on Ultra Wideband Systems and Technologies, Reston, VA, USA, 16–19 November 2003; pp. 1–9.
49. Park, Z.; Li, C.; Lin, J. A Broadband Microstrip Antenna With Improved Gain for Noncontact Vital Sign Radar Detection. *IEEE Antennas Wirel. Propag. Lett.* **2009**, *8*, 939–942. [CrossRef]
50. Tang, T.; Chuang, Y.; Lin, K. A Narrow Beamwidth Array Antenna Design for Indoor Non-contact Vital Sign Sensor. In Proceedings of the IEEE International Symposium on Antennas and Propagation, Chicago, IL, USA, 8–14 July 2012; pp. 1–2.
51. Lv, H.; Liu, M.; Jiao, T.; Zhang, Y.; Yu, X.; Li, S.; Jing, X.; Wang, J. Multi-target Human Sensing via UWB Bio-radar Based on Multiple Antennas. In Proceedings of the IEEE International Conference of IEEE Region 10 (TENCON 2013), Xian, China, 22–25 October 2013; pp. 1–4.

52. Mattia, V.D.; Petrini, V.; Pallotta, E.; Leo, A.D.; Pieralisi, M.; Manfredi, G.; Russo, P.; Primiani, V.M.; Cerri, G.; Scalise, L. Design and Realization of a Wideband Antenna for Non-contact Respiration Monitoring in AAL Application. In Proceedings of the IEEE/ASME 10th International Conference on Mechatronic and Embedded Systems and Applications (MESA), Senigallia, Italy, 10–12 September 2014; pp. 1–4.
53. Li, C.; Xiao, Y.; Lin, J. Design Guidelines for Radio Frequency Non-contact Vital Sign Detection. In Proceedings of the 29th Annual International Conference of the IEEE Engineering in Medicine and Biology Society, Lyon, France, 23–26 August 2007; pp. 1651–1654.